On principal features of organic electrolyte molecules in lithium ion battery performance

Tsuneda, Takao
Tateyama, Yoshitaka

(Citation)
Physical Chemistry Chemical Physics,21(41):22990-22998

(Issue Date)
2019-11-07

(Resource Type)
journal article

(Version)
Accepted Manuscript

Key features of organic electrolyte molecules in lithium ion battery

Takao Tsuneda[1*] and Yoshitaka Tateyama[2,3]
[1]*Graduate School of Science, Technology,*
and Innovation, Kobe University, Kobe 657-8501, Japan
[2]*Global Research Center for Environment and*
Energy based on Nanomaterials Science (GREEN),
National Institute for Materials Science (NIMS), Tsukuba 305-0044, Japan and
[3]*Center for Materials Research by Information Integration (CMI2),*
Research and Services Division of Materials Data and Integrated System (MaDIS),
National Institute for Materials Science (NIMS), Tsukuba 305-0047, Japan

Abstract

The lithium (Li) complexes of organic electrolyte solvents are theoretically investigated using the long-range correction for density functional theory in order to figure out the cause for the high performance of cyclic carbonate electrolytes in lithium ion battery (LIB). Calculating the Li complexes with ethylene carbonate solvent molecules proves that ten ligand molecules should be incorporated to obtain near-degenerate four- and five-coordination optimum structures and dramatically-improved orbital energies. The geometry optimizations of the Li complexes with thirteen types of organic solvent molecules give four-coordination neutral and five-coordination cation complexes for many solvent molecules. The five-coordination Li complexes are considered to use the Berry pseudorotation to approach the electrodes from Li atom. Calculating Koopmans, vertical and adiabatic ionization potentials and electron affinites shows that near-degeneracy and structural deformation effects play significant roles in the electronic states of the Li complexes. Mulliken charge and dipole moment analyses indicate that the Li complexes of cyclic carbonates construct deep electric double layer near electrodes due to the electron-donating ability of the ligand molecules. Molecular orbital analyses also explain that the Li complexes of cyclic carbonates easily construct solid electrolyte interface, which contributes to Li ion conductance, by localizing the accepted electron to one ligand molecule. In conclusion, the Li complexes of cyclic carbonates have three main features: preference of five-coordination structures, high electron-donating ability of ligand molecules, and localization of accepted electron into one ligand molecule.

I. INTRODUCTION

Lithium ion battery (LIB) is a rechargeable battery using lithium (Li) ion conductance between electrodes.[1,2] In LIB, Li ions transfer with ligand molecules from the cathode,[3] e.g., carbon graphite, to the anode, e.g., lithium cobalt oxide ($LiCoO_2$), when discharging and its backward when charging, by the medium of the separator, where Li salt such as lithium hexafluorophosphate ($LiPF_6$) and organic electrolyte solvent are impregnated in porous polymers such as polyethylenes.[4] The organic electrolyte solvent should meet the following major requirements:

1. High ionic conductivity that demands both the high dielectric constant according to the Born equation[5] and low viscosity due to the dependence on electric mobility for solvent,
2. High electrochemical and thermal stabilities that indicate the wide potential window of electrolyte molecules,[6] and
3. High-quality solid electrolyte interface (SEI) formation[7,8] that blocks the decomposition of electrolytes and even supports the Li ion conduction.

Since the high dielectric constant is incompatible with the low viscosity, the mixture of high dielectric solvent (or materials) and low viscosity solvent is usually used in the organic electrolyte solvent: As the high dielectric solvent (or materials), cyclic carbonates like ethylene carbonate (EC) and propylene carbonate (PC) are mainly used, while dimethyl carbonate (DMC), diethyl carbonate (DEC) and so forth are used as the low viscosity solvent. These cyclic carbonates have wider potential windows than that of aqueous solvents, though the window widths are insufficient unless the SEI is formed. The SEI is formed near the graphitic cathode and supports the Li ion conduction. It is known that better SEI is generated in EC solvent than in PC solvent under the use of graphite anode and it is improved by adding easily reducible vinyl carbonate (VC) and fluoroethylene carbonate (FEC). The development of innovative electrolyte solvents have long been addressed, because it leads directly to the development of breakthrough high-performance LIB.[8] However, it now reaches the ceiling. The best way to break the ceiling is to figure out the determining features of the electrolyte performance theoretically.

Based on many studies on the LIB performance,[9,10] the most probable bottleneck is considered to be the Li-Li bond formation in between electrolyte/cathode interface. Li ions approach the cathode like $LiCoO_2$, then make a chemical bond with Li metal in the cathode, and finally separates ligand organic electrolyte molecules. Assuming that this Li-Li bond formation is the main bottleneck process, the LIB performance is considered to depend on the following features:

1. Accessibility of Li complexes to the active sites of the cathode,
2. Electron acceptability of Li ions in the complexes, and
3. Ligand detachment ability after forming the Li-Li bonds.

The access of Li complexes consists of two significant processes: the diffusion of Li complexes inside the narrow channels of the cathode[11] and the subsequent approach of the complexes to the Li metal part of the cathode. The former process is explained by the electrophoretic migration of colloidal Li ion complexes inside the cathode channels of 100 - 1000 nm in diameter.[12] In this process, the performance should depend on the size and charge of the colloidal Li ion complexes. The latter process, on the other hand, may depend on the structure and charge distribution of unimolecular Li complexes, because the ligand molecules toward the cathode are expected to block the Li-Li bond formation and the positively-charged part of the complexes are presumed to approach the negatively-charged surface of the cathode. This implies that the Li complexes should have large dipole moments with allocating Li ions at the edges. The electron acceptability of Li ions is expected to depend on the electron distribution of the LUMOs of the cations (or more properly, the SOMOs of the neutrals) and the reaction barriers for the Li-Li bond formations in the complex/cathode interface.[13–15] After forming the Li-Li bonds, the ligand molecules should be detached from the Li atom. This process depends on the binding energies of the ligand molecules to the Li atom binding Li metal inside the cathode. To make clear the determining features of the LIB performance, it is important to explore the relationship between these dependence and the electrolyte performance.

Many theoretical studies have so far focused on the SEI formation (electrolytic decomposition), molecular dynamics (MD) of Li ion and chemical properties of the LIB electrolyte. For the SEI formation, the decomposition mechanisms of electrolyte molecules are explored for the addition of an electron,[16] Li atom,[17] and counter anions.[18] The *ab initio* MD simulations of the SEI formation are also performed for various electrolyte molecules[19] and for their decomposition on the graphitic anode.[20] For the *ab initio* MD simulations, static and dynamical properties of electrolyte solvent[21] and electron tunneling and oxidation on the cathode[20] are also carried out. The classical MD simulation of electric double layer formation is also performed under several electric voltage levels.[22] Recently, the relationships of chemical properties and molecular electronic properties are comparatively studied for various electrolyte molecules: activation energies vs unimolecular de-solvation energies,[23] oxidation potentials vs hardnesses,[24] and melting points vs coordination energies.[25] These theoretical studies have revealed the decomposition mechanisms, the microscopic structures of electrolytes and the determining features of several properties. However, the determining features of the electrolyte performance have not sufficiently been investigated to reveal the difference in the performance of electrolyte solvents.

In this study, we figure out the difference in the geometrical and electronic structures of various organic electrolyte solvents constructing the Li complexes in order to make clear the reason why cyclic carbonate solvents give high performance except for the electric mobility. We investigate the geometrical structures of the Li complexes by explicitly including ten organic solvent molecules, which are found to be required to model the Li complexes in organic solvents. For the electronic structures of the Li complexes, we apply the long-range correction[26,27] for density functional theory[28,29] (LC-DFT), which quantitatively provides the accurate orbital energies of small molecules.[29–31] Based on the results, we discuss about the requirements for organic electrolyte solvents to develop high-performance LIB electrolytes.

II. COMPUTATIONAL DETAILS

Calculations of the Li complexes have been performed for thirteen organic molecules, which are classified into three types: cyclic carbonate molecules, low dielectric constant molecules and high dielectric constant molecules. We have examined above-mentioned EC, PC, VC and FEC molecules as cyclic carbonate molecules, while we chose 1,2-dimethoxyethane (DME), 3-dioxolane (DOL), tetrahydrofuran (THF), ethyl methylcarbonate (EMC) and DMC molecules as low dielectric constant molecules and trimethyl phosphate (TMP), dimethyl sulfoxide (DMSO), acetonitrile (AN) and adiponitrile (APN) molecules as

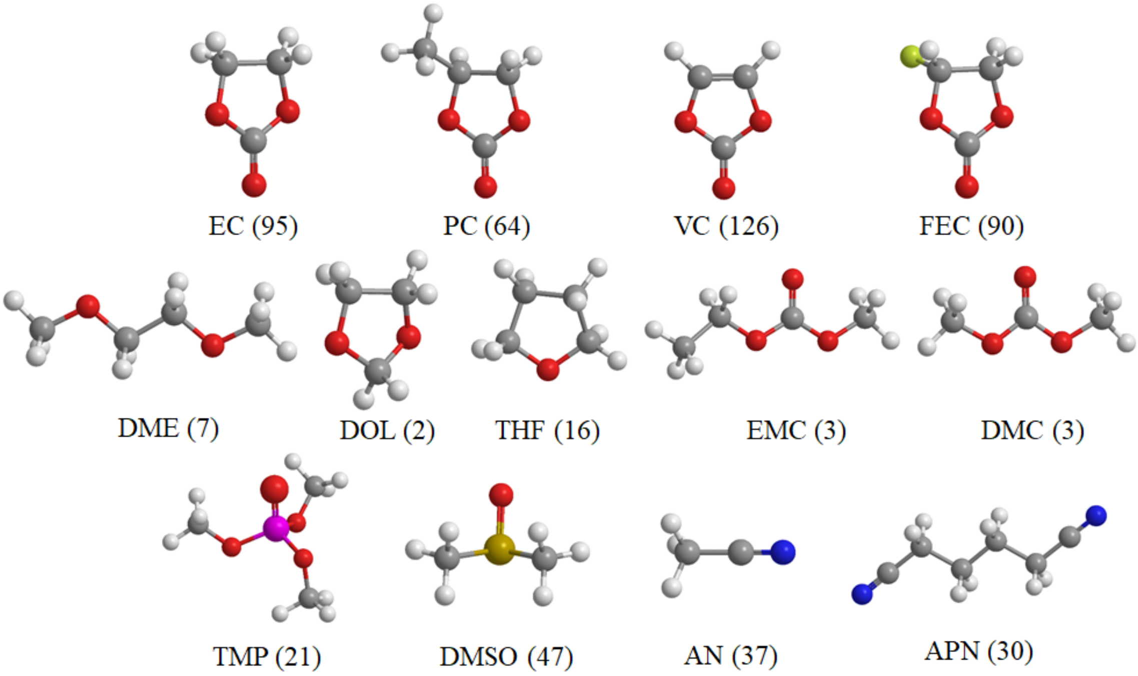

FIG. 1: Calculated organic solvent molecules. The numbers in the parentheses indicate the experimental dielectric constants.

high dielectric constant molecules (Fig. 1). For the Li complex of APN molecules, we have examined single- and double-coordination structures, in which two and four APN molecules are coordinated to Li ion by the cyano groups in the four-coordination complexes, respectively.

Geometry optimizations have been carried out by the Kohn-Sham calculations[28,29] using the long-range correction[26,27] for Becke 1988 exchange[32] plus Lee-Yang-Parr correlation[33] (LC-BLYP) functional (the only parameter $\mu = 0.33$[34]). The cc-pVDZ basis set[35,36] was used for all atoms. As a solvent effect, the polarizable continuum model[37] of water was included. In the geometry optimizations, several initial structures have been examined to find out the optimum geometries.

The Gaussian 09 suite of program[38] has been used to perform all the geometry optimizations and all the calculations of chemical properties including Mulliken populations and dipole moments. All of the optimized structures have been checked to ensure that they yield positive, real frequencies. The calculated results have been analyzed using Chemcraft version 1.8.[39]

III. CALCULATED RESULTS AND DISCUSSIONS

A. Lithium complex of ethylene carbonate solvent molecules

First, we explored the Li complex with EC solvent molecules for the orbital energies of the neutral complex with three numbers of the explicitly-incorporated organic solvent molecules and for the optimum coordination numbers of the neutral and monovalent and divalent cation complexes with ten organic solvent molecules in order to verify the calculation models of the Li complexes in solution.

Figure 2 displays the orbital energies of the neutral Li complexes with explicitly incorporating six, eight and ten EC solvent molecules: i.e., Li(EC)$_6$, Li(EC)$_8$ and Li(EC)$_{10}$, respectively. The figure clearly shows that the calculated orbital energies dramatically change from eight to ten EC solvent molecules. Note that four- and five-coordination complexes are calculated to have close total energies for the Li(EC)$_{10}$ complex as mentioned later, while only the four-coordination complexes are stable for the Li(EC)$_6$ and Li(EC)$_8$ complexes. The orbital energies of both the four- and five-coordination Li(EC)$_{10}$ complexes are, therfore, compared in the figure. As clearly shown in the figure, the orbital energies of these four- and five-coordination complexes are close to each other. This indicates that the orbital energies of the Li complexes depend not on the coordination number but on the number of organic solvent molecules. Moreover, this suggests that ten organic solvent molecules are required to model the Li complexes in solution, though some previous studies have adopted models with only four or less organic solvent molecules, which are the minimum to model Li ion complexes.[23–25] Hereafter, we, therefore, calculate the Li complexes with ten organic solvent molecules.

The optimized geometries of the neutral and monovalent and divalent cation Li(EC)$_{10}$ complexes are illustrated in Fig. 3. Note that the geometry optimizations are carried out setting their eight-coordination complexes as the initial geometries. As mentioned before, the four- and five-coordination complexes have close total energies for the neutral complexes; the former is 3.16 kcal/mol more stable than the latter in the total energies. On the other hand, we found that the optimum structures are five-coordination ones for both the monovalent and divalent cation Li(EC)$_{10}$ complexes. This result casts doubt on conventional calculation models that assume four-coordination structures for Li cation complexes.

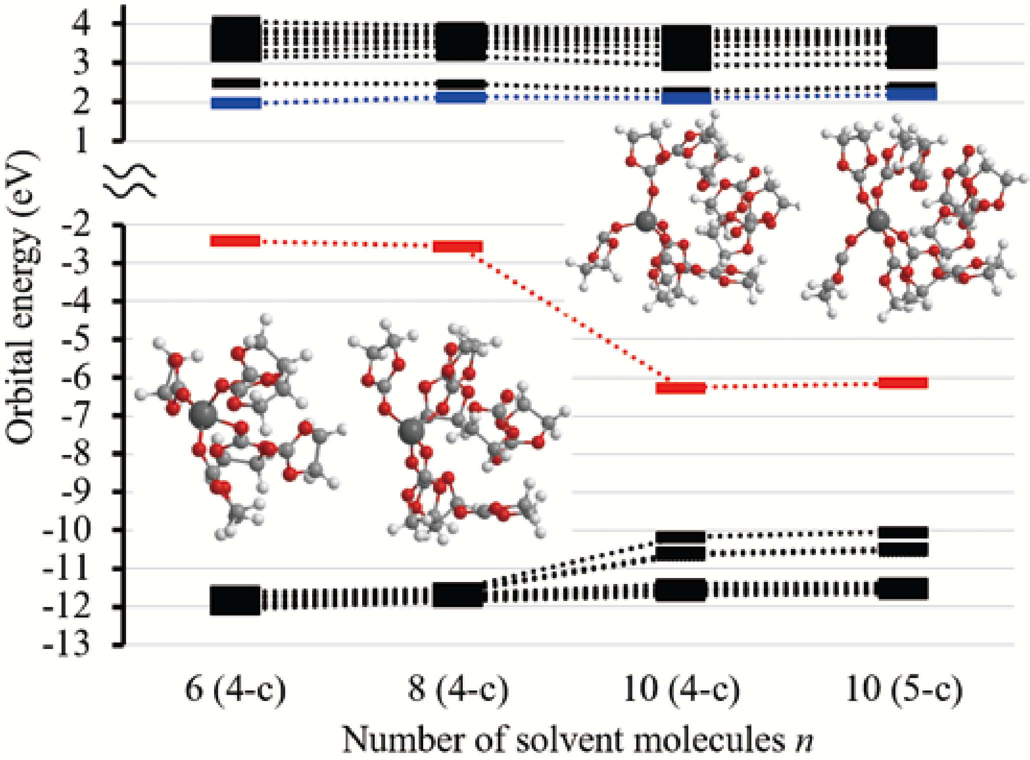

FIG. 2: Valence orbital energies of lithium complexes with ethylene carbonate (EC) molecules, Li(EC)$_n$ (the total numbers of EC molecules $n = 6$, 8 and 10). The levels of HOMOs and LUMOs are colored red and blue, respectively. In the parenthese attaching the total numbers of EC molecules, the coordination numbers are also shown like "4-c" for the four-coordination. LC-BLYP/cc-pVDZ is used.

B. Optimum geometries of lithium complexes with various organic solvent molecules

Next, we determined the optimum structures of Li complexes with ten organic solvent (S) molecules, i.e., LiS$_{10}$, focusing on which of four- and five-coordination structures these complexes take, on the basis of the results in Sec. III. The optimum structure images and their Cartesian coordinates are given in the supporting information. Table I summarizes the optimum coordination numbers of LiS$_{10}$ complexes for thirteen types of organic solvent molecules. As shown in the table, the optimum coordination numbers significantly depend on the types of of the organic solvent molecules and the cyclic carbonate molecules tend to take five-coordination structures for the cations. Note that the four-coordination structures

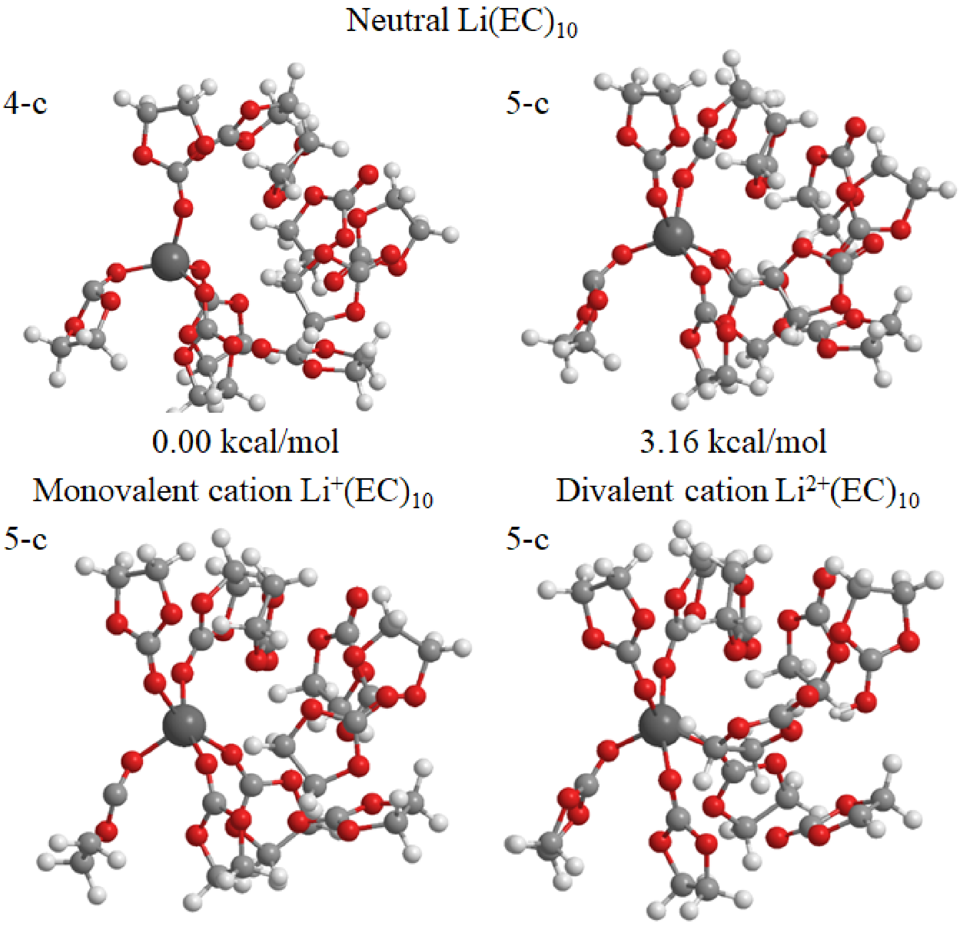

FIG. 3: Optimized structures of lithium complexes with ethylene carbonate (EC) molecules, for three types of charges: neutral Li(EC)$_{10}$, monovalent cation Li$^+$(EC)$_{10}$ and divalent cation Li^{2+}(EC)$_{10}$. The coordination numbers are also shown like "4-c" for the four-coordination. For the neutral complex, the optimized structures of both 4-c and 5-c complexes are shown with the energy difference, for comparison. LC-BLYP/cc-pVDZ is used.

for the Li complex cations of AN and APN-1 are supposed to be due to the insufficient models, because the five-coordination structures of these complexes are supposed to give very large dipole moments or very large steric effects, respectively. This suggests that the five-coordination structures of the neutral Li(VC)$_{10}$ and Li(FEC)$_{10}$ complexes and the four-coordination structures of the cation Li(EMC)$_{10}$, Li(DMC)$_{10}$ and Li(APN-2)$_{10}$ complexes are exceptional in the LiS$_{10}$ complexes. We, therefore, consider that the Li complexes basically take the four-coordination structures for the neutrals and the five-coordination structures of the cations, though these four- and five-coordination structures may be mixed at some

TABLE I: Optimum coordination numbers of lithium complexes with ten solvent molecules, LiS_{10}, for thirteen types of organic solvent molecules with three types of charges: neutral (0), monovalent cation (+1) and divalent cation (+2).

Organic solvent	Coordination number 0	+1	+2
EC	4	5	5
PC	4	5	5
VC	5	5	5
FEC	5	5	5
DME	4	5	5
DOL	4	5	5
THF	4	5	5
EMC	4	4	4
DMC	4	4	4
TMP	4	5	5
DMSO	4	5	5
AN	4	4	4
APN-1	4	4	4
APN-2	4	4	4

rate in actual electrolytes due to their close energies. The unique optimum structures may contribute to the performance of these Li complexes as LIB electrolytes.

It is interesting to note that five-coordination structures enable complexes to proceed Berry pseudorotation. Figure 4 illustrates the schematic diagram of the Berry pseudorotation. As the figure shows, five-coordination complexes can switch between square pyramidal (Sp) and trigonal bipyramidal (Tb) structures. The figure implies that the Sp structure facilitates to approach electrodes from the opposite side of the apical ligand molecule ($\mathrm{L_a}$). That is, the Li complex cations of the optimum five-coordination structures easily approach the electrodes by taking the Sp structures and then transform to the four-coordination structures after accepting an electron from the electrodes. As mentioned in Sec. I, it is known

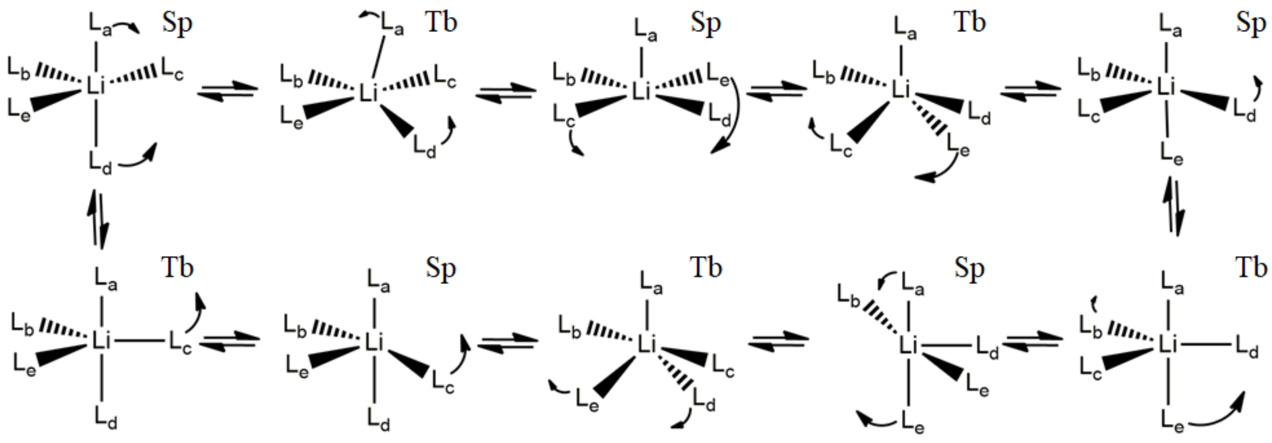

FIG. 4: Schematic diagram of Berry pseudorotation of lithium complex with five-coordination ligand molecules, LiL_5. "Sp" and "Tb" indicate square pyramidal and trigonal bipyramidal structures.

that VC and FEC, which are calculated to take five-coordination even for the neutral Li complexes, are easily reduced and are mixed in EC and PC solvents to improve the performance. We, therefore, consider that the five-coordination Li complexes take advantage of this Berry pseudorotation to improve their performances as LIB electrolytes.

C. Koopmans, vertical and adiabatic ionization potentials and electron affinities of lithium complexes with various organic solvent molecules

It is also interesting to focus on the ionization potentials (IPs) and electron affinities (EAs) of the Li complexes, because the oxidation potentials of the Li complexes are known to depend on their hardnesses, which are the halves of the HOMO-LUMO gaps.[24] Figure 5(a) compares the calculated Koopmans, vertical and adiabatic IPs and EAs of the Li complexes with ten organic solvent molecules, LiS_{10}. The Koopmans IPs and EAs indicate the minus HOMO and minus LUMO energies, respectively. The figure shows that the Koopmans IPs and EAs are overestimated in comparison with the vertical IPs and EAs. Figure 5(b) plots the difference between the Koopmans and vertical IPs and between the Koopmans and vertical EAs. As the figure shows, the errors of the Koopmans IPs and EAs are close to 2 eV for all organic solvent molecules except for the EAs of EMC, DMC and DOL molecules. This implies that the errors are attributed to the overestimated energy splittings probably

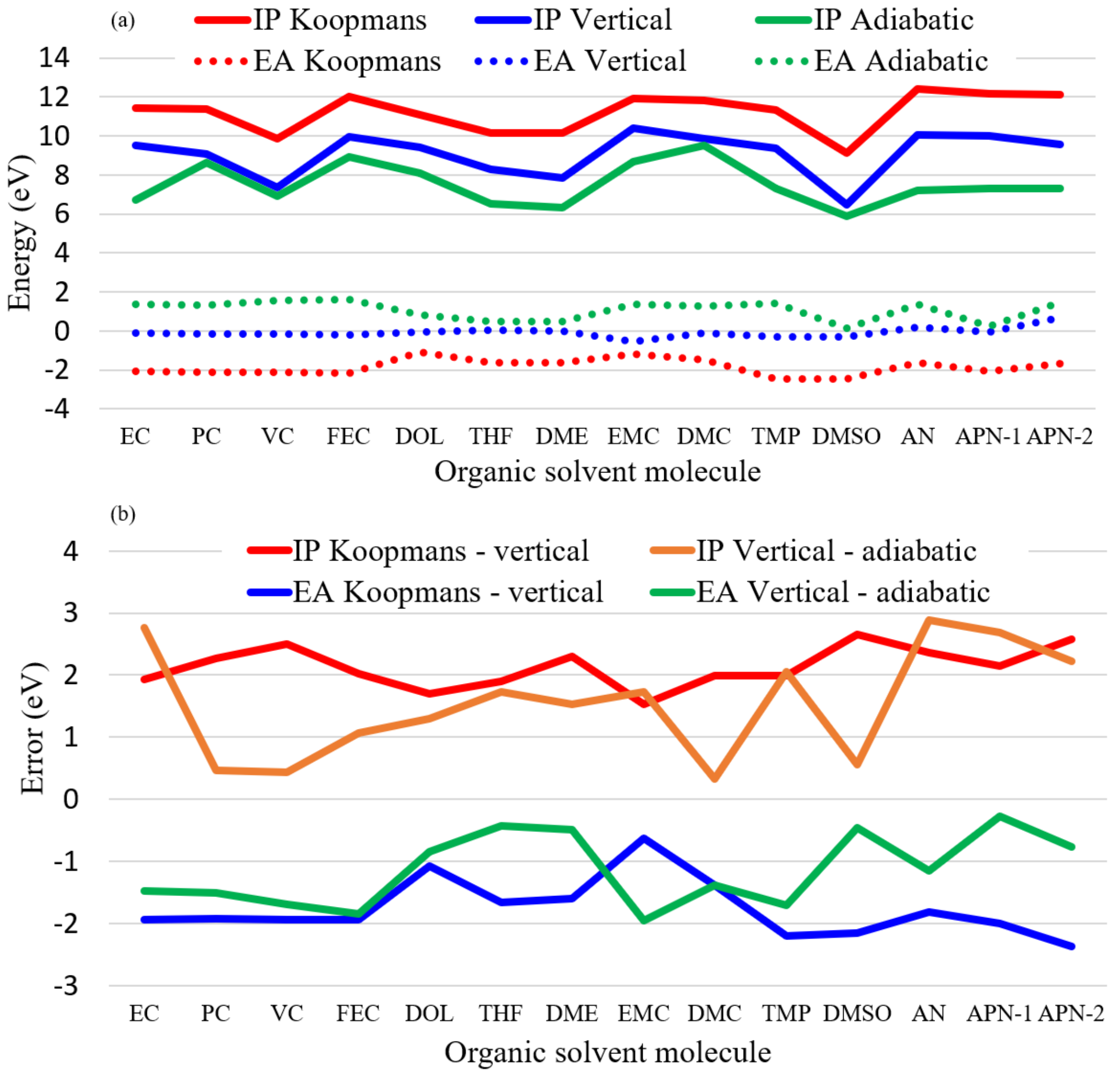

FIG. 5: Calculated Koopmans, vertical and adiabatic ionization potentials (IPs) and electron affinities (EAs) of lithium complexes, LiS$_{10}$, for thirteen types of solvent (S) molecules: (a) The Koopmans, vertical and adiabatic IP and EA values and (b) the difference between the Koopmans and vertical values and between the vertical and adiabatic values for the IPs and EAs. Koopmans IPs and EAs correspond to the minus signs of HOMO and LUMO energies. The geometries of the neutral and divalent cation systems are fixed at the optimum geometries of the monovalent cation systems in the vertical IP and EA calculations, while these geometries are optimized in the adiabatic calculations. LC-BLYP/cc-pVDZ is used.

due to the large long-range exchange interactions between the HOMOs and LUMOs. We consider that the large long-range exchange interactions come from the neglect of near-degeneracy effects, which are essentially excluded in single-configuration methods such as DFT.[29] This is because these complexes have many near-degenerate orbitals for HOMOs (e.g., the HOMO−11 through HOMO−1 energies of the $Li(EC)_{10}$ complex are calculated in the range of 0.5 eV from the HOMO energy), indicating that they have many low-lying near-degenerate electronic states. Note that the incorporation of the near-degeneracy effects in multiconfigurational methods,[29] tend to decrease the excitation energies. We, therefore, suggest that these Li complexes have significant near-degeneracy effects in organic solutions.

Figures 5 also indicates that these Li complexes have considerable structural deformation effects. The difference of the vertical and adiabatic IPs and EAs in Fig. 5(b) shows that the structural deformation effects on the IPs and EAs are $0.5 \sim 3.0$ eV and $0.5 \sim 2.0$ eV, respectively, and significantly depend on the species of organic solvent molecules. The largest structural deformation effects on IPs and EAs are given for the complexes with EC and AN solvent molecules and for the complexes with EMC and FEC solvent molecules, respectively. Note that the importance of the structural deformation effects after electron transfers has been emphasized following the Marcus theory.[40] This result, therefore, indicates that the structural deformation effects should also be taken into consideration for investigating the electronic states of the Li complexes after electron transfers.

D. Mulliken charge and dipole moment analyses of lithium complexes with various organic solvent molecules

The Mulliken charges and dipole moments of the Li complexes are also useful in considering the state and mobility of the complexes in organic solution. Figure 6 displays the calculated Mullken charges of (a) Li, (b) ligand molecules and (c) the Li complexes including them. As shown in Fig. 6(a), the charge of Li atom in the complexes are calculated to be slightly negative even for most cations. This may be partly due to the insufficient number of organic solvent molecules, because the Li charge of neutral $Li(EC)_6$ and $Li(EC)_8$ complexes in Sec. III A are calculated to be -1.017 and -1.002, respectively, while that of the $Li(EC)_{10}$ complex is -0.522. This result supports that ten or more organic solvent molecules are required in calculation models to investigate the electronic structures of the Li complexes in

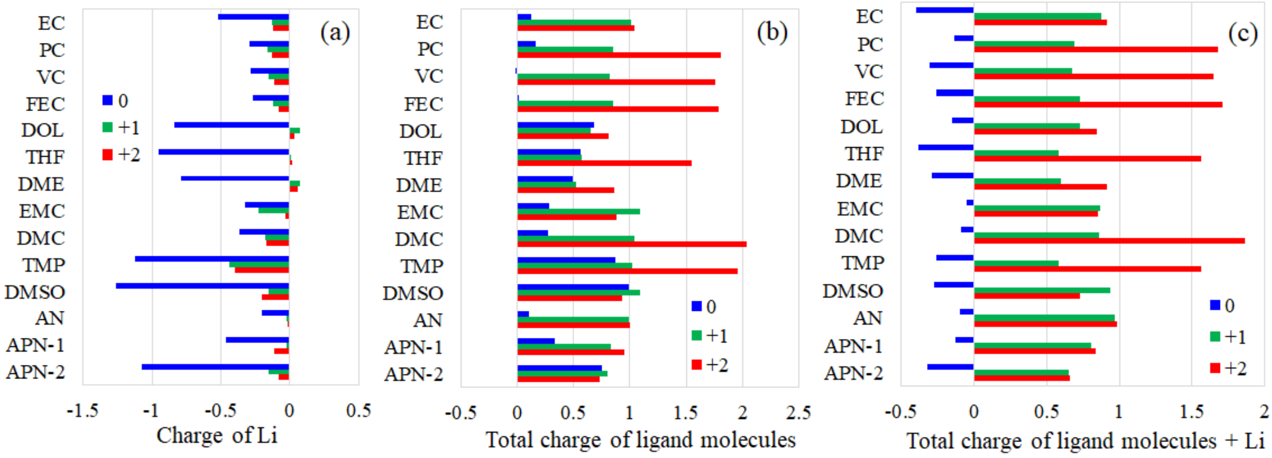

FIG. 6: Calculated Mulliken charges of (a) lithium, (b) ligand molecules and (c) lithium plus the ligand molecules of the lithium complexes, LiS_{10}, for thirteen types of solvent (S) molecules with three types of charges: neutral (0), monovalent cation (+1) and divalent cation (+2). LC-BLYP/cc-pVDZ is used.

organic solutions. Moreover, Figs. 6(b) and (c) indicate that the total charges of the Li complexes are positive (close to +1 for the monovalent cations) due to the ligand molecules with considerable positive charges. This indicates that the monovalent cation Li complexes transfer as the monovalent ions in solution even though the Li has negative charge.

Figure 6 also indicates that the Mulliken charges significantly depend on the species of the organic solvent molecules. In particular, the Li atom of the neutral complexes and the ligand molecules of the divalent cation complexes provide very different charges dependent on the species of organic solvents. These results are related to the electron-donating and -accepting regions and abilities of the Li complexes. The figures show that the Li complexes of DMSO, TMP, APN-2, THF, DOL and DME easily accept an electron in the Li atom, while those of the cyclic carbonates (EC, PC, VC and FEC), EMC, DMC and AN easily donate an electron from the ligand molecules. It is interesting to note that the former complexes provide five-coordination structures as the optimum ones of the cations except for APN-2, while EMC, DMC and AN give four-coordination structures as the optima except for the cyclic carbonates, as shown in Table I. This result implies the unique nature of the cyclic carbonates, which give the optimum five-coordination Li cation complexes despite of the high electron donating ability from the ligand molecules. We consider that this unique nature may be related to the high performance of the Li complexes of the cyclic carbonates.

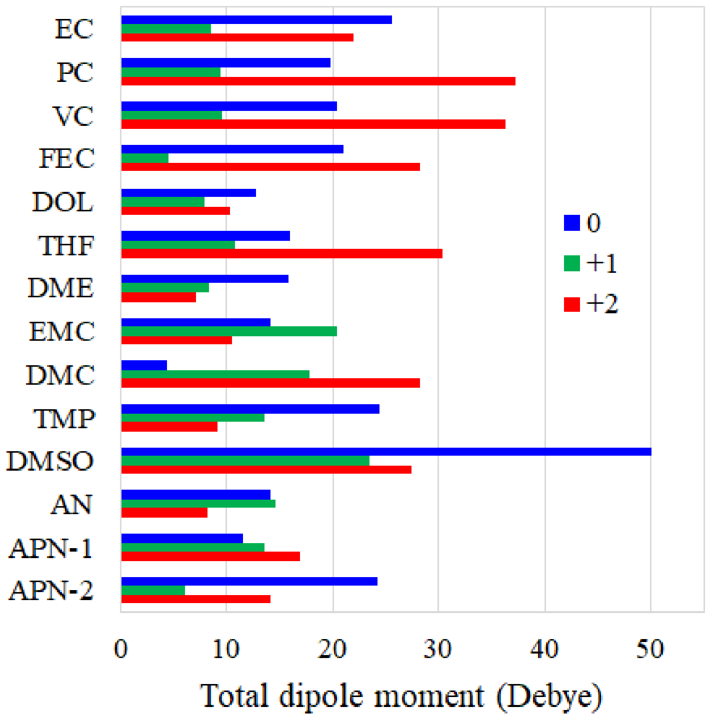

FIG. 7: Calculated total dipole moments of the lithium complexes, LiS_{10}, for thirteen types of solvent (S) molecules with three types of charges: neutral (0), monovalent cation (+1) and divalent cation (+2). LC-BLYP/cc-pVDZ is used.

Dipole moments are also useful to discuss the electric double layer, which is generated by the Li complexes and is expected to support the transfer of the complexes. Figure 7 plots the calculated total dipole moments of the Li complexes with various organic solvent molecules, LiS_{10} for the neutral, monovalent and divalent cations. As the figure shows, the dipole moments significantly depend on the species of the organic solvent molecules. Compared to Fig. 6, the dipole moments seem to have no close relation to the total charges of the complexes. The neutral and divalent cation Li complexes of the cyclic carbonates give larger dipole moments than those of many other organic solvent molecules. This may suggest that the cyclic carbonates construct deeper electric double layer than others in the vicinity of the anode and cathode, because electrons transfer at the electrodes.

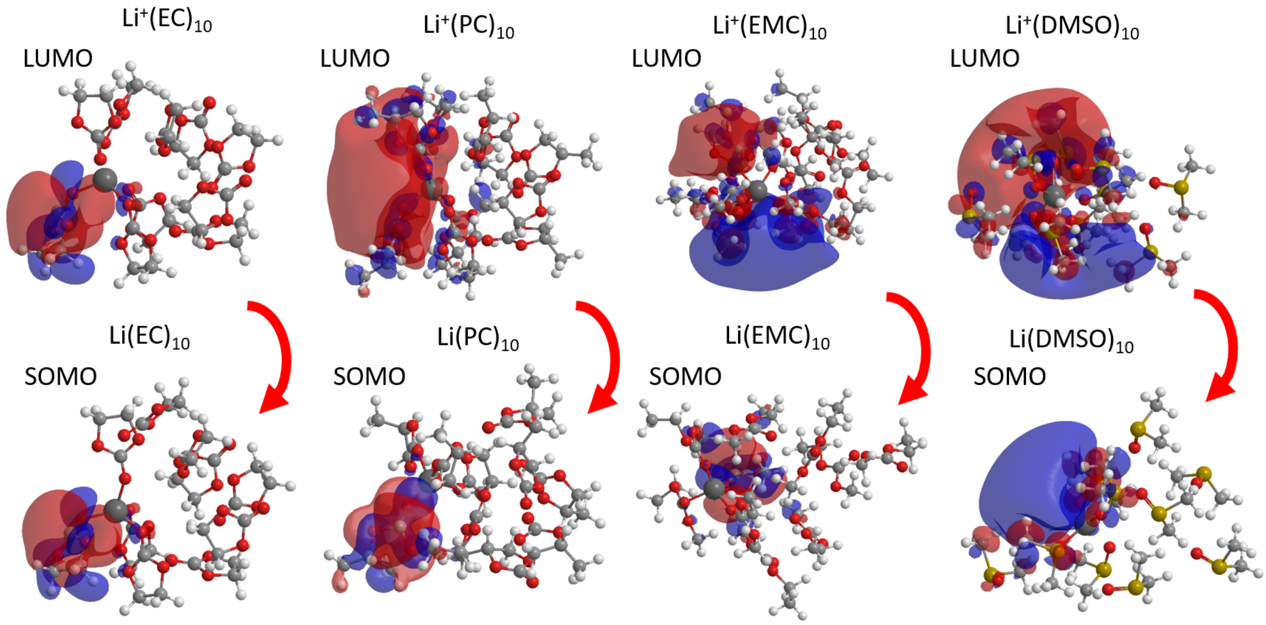

FIG. 8: Calculated LUMO images of the monovalent cation Li^+S_{10} complex and SOMO images of the neutral LiS_{10} complex, which correspond to the orbitals before and after accepting an electron, for four types of solvent (S) molecules: ethylene carbonate (EC), propylene carbonate (PC), ethyl methylcarbonate (EMC) and dimethyl sulfoxide (DMSO). LC-BLYP/cc-pVDZ is used.

E. Molecular orbital analyses of lithium complexes with various organic solvent molecules

Finally, let us explore the molecular orbital transformations of the Li complexes with various organic solvent molecules before and after accepting an electron. Figure 8 illustrates the molecular orbital images for the LUMOs of the monovalent cations and the SOMOs of the neutrals for four types of the organic solvent molecules, EC, PC, EMC and DMSO. For all calculated organic solvent molecules, these LUMO and SOMO images are presented in Fig. S2 of the supporting information. In Fig. 8, an electron is found to be occupied in the ligand molecule at the edge of the monovalent cation complexes of EC and PC even after the structural relaxation of their neutral complexes, though the electron is delocalized over a few ligand molecules in the Li complexes of EMC and DMSO. Similar electron occupancy is found for the Li complexes of VC, FEC and AN (see Fig. S2 of the supporting information). Note that the coordination number of the $Li(AN)_{10}$ complex is considered to depend on the number of the solvent molecules, as mentioned before. This result, therefore, clearly explains why the high decomposition rate of the Li complex is given for the cyclic carbonate solvents. For other solvent molecules, the LUMOs of the monovalent cations are widely delocalized over a few ligand molecules in the edge sides and the SOMOs of the neutrals are shrank but remain delocalized in a few ligand molecules. As mentioned in Sec. I, the SEI, which is formed near the cathode after the decomposition, is supposed to contribute to the increase in the Li ion conductance. We, therefore, conclude that the high performance of the Li complexes of ethylene carbonates is also attributed to the electron localization of the SOMOs after accepting an electron from the cathode.

IV. CONCLUSIONS

In this study, we have comparatively investigated the Li complexes of organic solvent molecules in order to make clear the reason why cyclic carbonates provide better electrolyte performance in Li ion battery (LIB). Using the Li complex models with ten organic solvent molecules and the long-range correction (LC) for density functional theory (DFT),[26,27] we have explored the coordination structures, molecular orbital energies, and molecular orbital images of the Li complexes. Consequently, we have succeeded to find out the unique features of the Li complexes of the cyclic carbonates, which contribute to the high performance in LIB.

First, we have explored the Li complexes with three numbers of EC solvent molecules, n = 6, 8 and 10, for the optimum geometries and the orbital energies. As a result, we have found that four- and five-coordination structures are obtained as near-degenerate optimum geometries only for the Li complex with ten EC molecules, $\mathrm{Li(EC)_{10}}$. We have also found that the orbital energies of the Li complex dramatically change from $n = 8$ to $n = 10$. These results indicate that ten solvent molecules are required at least to model the Li complex in organic solvents and that they provide near-degenerate four- and five-coordination optimum structures.

Next, we have optimized the Li complex geometries for various types of organic solvent molecules. We have consequently found that the Li complexes of many organic solvents provide four-coordination structures for the neutrals and five-coordination ones for the cations as the optima, while the optimum neutral complexes of VC and FEC have five-coordination and the optimum cation complexes of EMC, DMC and APN-2 have four-coordination. The five-coordination complexes lead to the Berry pseudorotation, in which the complexes switch between square pyramidal (Sp) and trigonal bipyramidal (Tb) structures. The Li complexes in the Sp structure are considered to easily approach electrodes from the opposite side of the apical ligand molecule. It is, therefore, concluded that many Li complexes take advantage of the Berry pseudorotation to approach the electrodes.

We have also compared the Koopmans, vertical and adiabatic ionization potentials (IPs) and electron affinities (EAs) to figure out the relation between the HOMO-LUMO gaps and the performance of the Li complexes. The Koopmans IPs and EAs correspond to the HOMO and LUMO energies, respectively. As a result, we have found that the present LC-

DFT calculations give large discrepancies for both the differences between the Koopmans and vertical IPs and EAs and between the vertical and adiabatic IPs and EAs. We have considered that the former difference comes from the neglect of near-degeneracy effects in single-configurational DFT calculations and the latter difference stems from the structural deformation effects after electron transfers following the Marcus theory.

The Mulliken charge and dipole moment analyses have also been carried out for the Li complexes in order to explore the electronic states and the mobilities of these complexes. Consequently, we have found that for most organic solvents, the charge of Li atom in the complexes are slightly negative even for most cations, while the charges of the Li complexes are close to +1. The results also show that the Li atom of the neutral complexes and the ligand molecules of the divalent cation complexes give very different charges dependent on the species of the organic solvents. Comparing the charges to the above-mentioned coordination structures, we have found that the complexes with large negative Li atom for the neutrals tend to have five-coordination structures for the cations, while the complexes with large positive ligand molecules tend to have four-coordination structures except for the cyclic carbonate complexes. We have also found that the neutral and divalent cation cyclic carbonate complexes have larger dipole moments than those of many other complexes. Considering these results, we suggest that the cyclic carbonate complexes construct deeper electric double layer than others in the vicinity of the electrodes.

Finally, we have focused on the molecular orbital transformations of the Li complexes before and after accepting an electron. As a result, we have found that the electron is occupied in the ligand molecule at the edge of the monovalent cation complexes for the cyclic carbonate complexes, though the electron is delocalized over a few ligand molecules for many other complexes even after the structural relaxations. This clearly explains why the cyclic carbonates easily construct solid electrolyte interface, which contributes to increase Li ion conductance.

In summary, we conclude that the Li complexes of cyclic carbonates have the following features in organic solutions:

1. Prefering five-coordination allowing the Berry pseudorotation, which becomes easily accessible from the Li atom to electrodes,

2. Possessing high electron-donating ability of ligand molecules, which supports to con-

struct deep electric double layer near electrodes, and

3. Localizing the accepted electron into one ligand molecule (at the edge of the layer), which facilitates the decomposition of the ligand molecule and makes it easy to form solid electrolyte interface.

ACKNOWLEDGMENTS

This study was supported by the Japanese Ministry of Education, Culture, Sports, Science and Technology (MEXT) (Grants: 17H01188). This study was also partly supported by MEXT as "Priority Issue on Post-K computer" (Development of new fundamental technologies for high-efficiency energy creation, conversion/storage and use).

SUPPLEMENTARY MATERIAL AVAILABLE

The images of the optimum geometries of Li complexes with 14 types of ten organic electrolyte molecules are given in Fig. S1 of the supporting information. The molecular orbital images of the LUMOs of the monovalent cations and the SOMOs of the neutrals are also shown for Li complexes with 14 types of ten organic electrolyte molecules in Fig. S2. This material is available free of charge via the Internet at xxxx.

FIGURE CAPTIONS

Fig. 1.
Calculated solvent molecules. The numbers in the parentheses are the experimental dielectric constants.

Fig. 2.
Valence orbital energies of lithium complexes with ethylene carbonate (EC) molecules, $\mathrm{Li(EC)}_n$ (the total numbers of EC molecules n = 6, 8 and 10). The levels of HOMOs and LUMOs are colored red and blue, respectively. In the parentheses attaching the total numbers of EC molecules, the coordination numbers are also shown like "4-c" for the four-coordination. LC-BLYP/cc-pVDZ is used.

Fig. 3.
Optimized structures of lithium complexes with ethylene carbonate (EC) molecules, for three types of charges: neutral $\mathrm{Li(EC)}_{10}$, monovalent cation $\mathrm{Li^+(EC)}_{10}$ and divalent cation $\mathrm{Li^{2+}(EC)}_{10}$. The coordination numbers are also shown like "4-c" for the four-coordination. For the neutral complex, the optimized structures of both 4-c and 5-c complexes are shown with the energy difference, for comparison. LC-BLYP/cc-pVDZ is used.

Fig. 4.
Schematic diagram of Berry pseudorotation of five-coordination lithium complex, LiL_5. "Sp" and "Tb" indicate square pyramidal and trigonal bipyramidal structures.

Fig. 5.
Calculated Koopmans, vertical and adiabatic ionization potentials (IPs) and electron affinities (EAs) of lithium complexes, LiS_{10}, for 14 types of solvent (S) molecules: (a) The Koopmans, vertical and adiabatic IP and EA values and (b) the difference between the Koopmans and vertical values and between the vertical and adiabatic values for the IPs and EAs. Koopmans IPs and EAs correspond to the minus signs of HOMO and LUMO energies. The geometries of the neutral and divalent cation systems are fixed at the optimum geometries of the monovalent cation systems in the vertical IP and EA calculations, while these geometries are optimized in the adiabatic calculations. LC-BLYP/cc-pVDZ is used.

Fig. 6.

Calculated Mulliken charges of (a) lithium, (b) ligand molecules and (c) lithium plus the ligand molecules of the lithium complexes, for thirteen types of solvent (S) molecules with three types of charges: neutral (0), monovalent cation (+1) and divalent cation (+2). LC-BLYP/cc-pVDZ is used.

Fig. 7.

Calculated total dipole moments of the lithium complexes, LiS_{10}, for 14 types of solvent (S) molecules with three types of charges: neutral (0), monovalent cation (+1) and divalent cation (+2). LC-BLYP/cc-pVDZ is used.

Fig. 8.

Calculated LUMO images of the monovalent cation $Li^{+}S_{10}$ complex and SOMO images of the neutral LiS_{10} complex, which correspond to the orbitals before and after accepting an electron, for four types of solvent (S) molecules: ethylene carbonate (EC), propylene carbonate (PC), ethyl methylcarbonate (EMC) and dimethyl sulfoxide (DMSO). LC-BLYP/cc-pVDZ is used.

---

* Electronic address: `tsuneda@phoenix.kobe-u.ac.jp`

[1] J. B. Goodenough and Y. Kim, Chem. Mater. **22**, 587 (2010).

[2] P. G. Bruce, B. Scrosati, and J.-M. Tarascon, Angew. Chem., Int. Ed. **47**, 2930 (2008).

[3] M. S. Whittingham, Chem. Rev. **104**, 4271 (2004).

[4] J. Gao, S.-Q. Shi, and H. Li, Chin. Phys. B **25**, 018210(1 (2016).

[5] M. Born, Z. Phys. **1**, 45 (1920).

[6] P. Peljo and H. H. Girault, Energy Environ. Sci. **11**, 2306 (2018).

[7] E. Peled, D. Golodnitsky, and G. Ardel, J. Electrochem. Soc. **144**, L208 (1997).

[8] S. J. An, J. Li, C. Daniel, D. Mohanty, S. Nagpure, and D. L. I. Wood, Carbon **105**, 52 (2016).

[9] K. Xu, Chem. Rev. **114**, 11503 (2014).

[10] M. Gauthier, T. J. Carney, A. Grimaud, L. Giordano, N. Pour, H. Chang, D. P. Fenning, S. F. Lux, O. Paschos, C. Bauer, et al., J. Phys. Chem. Lett. **6**, 4653 (2013).

[11] M. S. Islam and C. A. J. Fisher, Chem. Soc. Rev. **43**, 185 (2014).

[12] T. F. Fuller, M. Doyle, and J. Newman, J. Electrochem. Soc. **141**, 1 (1994).

[13] F. Sagane, T. Abe, Y. Iriyama, and Z. Ogumi, J. Power Sources **146**, 749 (2005).

[14] T. Abe, F. Sagane, M. Ohtsuka, Y. Iriyama, and Z. Ogumi, J. Electrochem. Soc. **152**, A2151 (2005).

[15] Y. Yamada, F. Sagane, Y. Iriyama, T. Abe, and Z. Ogumi, J. Phys. Chem. C **113**, 14528 (2009).

[16] X. Zhang, J. K. Pugh, and P. N. Ross, J. Electrochem. Soc. **148**, E183 (2001).

[17] Y. Wang, S. Nakamura, M. Ue, and P. B. Balbuena, J. Am. Chem. Soc. **123**, 11708 (2001).

[18] L. Xing, O. Borodin, G. D. Smith, and W. Li, J. Phys. Chem. A **115**, 13896 (2011).

[19] K. Ushirogata, K. Sodeyama, Y. Okuno, and Y. Tateyama, J. Am. Chem. Soc. **135**, 11967 (2013).

[20] K. Leung, J. Phys. Chem. C **117**, 1539 (2012).

[21] P. Ganesh, D. Jiang, and P. R. C. Kent, J. Phys. Chem. B **115**, 3085 (2011).

[22] O. Borodin, X. Ren, J. Vatamanu, A. v. W. Cresce, J. Knap, and K. Xu, Acc. Chem. Res. **50**, 2886 (2017).

[23] M. Okoshi, Y. Yamada, A. Yamada, and H. Nakai, J. Electrochem. Soc. **160**, A2160 (2013).

[24] M. Okoshi, A. Ishikawa, Y. Kawamura, and H. Nakai, ECS Electrochem. Lett. **4**, A103 (2015).

[25] K. Sodeyama, Y. Igarashi, T. Nakayama, Y. Tateyama, and M. Okada, Phys. Chem. Chem. Phys. **20**, 22585 (2018).

[26] T. Tsuneda and K. Hirao, WIREs Comput. Mol. Sci. **4**, 375 (2014).

[27] H. Iikura, T. Tsuneda, T. Yanai, and K. Hirao, J. Chem. Phys. **115**, 3540 (2001).

[28] W. Kohn and L. J. Sham, Phys. Rev. A **140**, 1133 (1965).

[29] T. Tsuneda, *Density Functional Theory in Quantum Chemistry* (Springer, Tokyo, 2014).

[30] T. Tsuneda, J.-W. Song, S. Suzuki, and K. Hirao, J. Chem. Phys. **133**, 174101 (2010).

[31] T. Tsuneda, Int. J. Quantum Chem. **115**, 270 (2015).

[32] A. D. Becke, Phys. Rev. A **38**, 3098 (1988).

[33] C. Lee, W. Yang, and R. G. Parr, Phys. Rev. B **37**, 785 (1988).

[34] Y. Tawada, T. Tsuneda, S. Yanagisawa, T. Yanai, and K. Hirao, J. Chem. Phys. **120**, 8425 (2004).

[35] T. H. Dunning Jr., J. Chem. Phys. **90**, 1007 (1989).

[36] R. A. Kendall, J. T. H. Dunning, and R. J. Harrison, J. Chem. Phys. **96**, 6796 (1992).

[37] J. Tomasi, B. Mennucci, and R. Cammi, Chem. Rev. **105**, 2999 (2005).

[38] M. J. Frisch, G. W. Trucks, H. B. Schlegel, G. E. Scuseria, M. A. Robb, J. R. Cheeseman, G. Scalmani, V. Barone, B. Mennucci, G. A. Petersson, et al., *Gaussian09 Revision D.01* (2009), gaussian Inc. Wallingford CT.

[39] G. Zhurko and D. Zhurko, Lite version build **8**, 2005 (2005).

[40] R. A. Marcus, J. Chem. Phys. **24**, 979 (1956).